JOURNAL OF Materials CHEMISTRY

Synthesis and characterisation of microporous bimetallic Fe–Cr–Si–O materials derived from silsesquioxane precursors

Nicolae Maxim,[a] Arian Overweg,[b] Patricia J. Kooyman,[c] Anton Nagy,[d] Rutger A. van Santen[a] and Hendrikus C. L. Abbenhuis*[a]

[a]*Schuit Institute of Catalysis, Eindhoven University of Technology, P.O. Box 513, 5600 MB Eindhoven, The Netherlands*
[b]*Interfacultair Reactor Instituut, Mekelweg 15, 2629 JB Delft, The Netherlands*
[c]*National Centre for HREM, Rotterdamseweg 137, 2628 AL Delft, The Netherlands*
[d]*Avantium Technologies B.V., Zekeringstraat 29, 1000 CX Amsterdam, The Netherlands.*
E-mail: H.C.L.Abbenhuis@tue.nl

Received 24th May 2002, Accepted 9th August 2002
First published as an Advance Article on the web 16th September 2002

Calcination of silsesquioxane mixtures of (c-C_5H_9)$_7$$Si_7O_9(OH)_3$, **1**, (c-$C_5H_9$)$_7$$Si_7O_{12}Fe(CH_3)_2N(CH_2)_2N(CH_3)_2$, **2**, and (c-$C_5H_9$)$_7$$Si_7O_9$$(OSiMe_3)O_2CrO_2$, **3**, led to microporous amorphous bimetallic Fe–Cr–Si–O materials with different Fe : Cr ratios. A set of complementary characterisation techniques including N_2 physisorption, XRD, XPS, RS, IR, HRTEM and Mössbauer spectroscopy were used to follow the variation of the textural properties, metal oxide dispersion and speciation with metal content. Fe–Cr–Si–O materials possess high surface areas and uniformly controlled micropores with an average pore size diameter of around 6–7 Å. Metal oxide speciation of calcined silsequioxane mixtures appears to be significantly different from that observed for these metals in the individually calcined metal silsesquioxanes. The iron oxide and monochromates are the predominant species in the calcined precursors **2** and **3** while very small particles (2–4 nm) of bimetallic mixed oxides are the major species in the Fe–Cr–Si–O materials. This suggests that the metal oxide species are highly interdispersed and can come into close contact with each other during the calcination procedure thus favoring the formation of the bimetallic mixed oxide phase. In contrast, a silica reference material containing 7% Fe and 3% Cr prepared *via* the impregnation method showed only chromate species and large particles (10–30 nm) of iron oxide. This suggests that metallasilsesquioxane mixtures may be used as versatile precursors for the preparation of silica-based catalysts containing very small and well dispersed particles of mixed metal oxides.

Introduction

The chemistry of silsesquioxanes has recently received considerable attention. This is due to the fact that these organosilicon compounds have been found to offer numerous exciting applications in materials science and catalysis. Metal-free silsesquioxanes are being used as precursors for ceramic materials[1] while metallasilsesquioxanes are being implemented as homogeneous model systems for silica-supported metal catalysts or metal-containing zeolites.[2] Metallasilsesquioxanes have been found to be active catalysts themselves.[3,4] Metal-containing silsesquioxanes have also been found to be convenient precursors for potentially catalytic microporous amorphous M–Si–O materials with high surface area, uniformly controlled micropores and high metal dispersion.[5] This latest development has been stimulated by the fact that in recent years numerous main group, early and late transition metal silsesquioxane complexes have become available.[6] The known literature already reports the calcination of Ti, Cr, Mg, Al and Ga silsesquioxanes in order to form microporous mixed oxides with catalytic activity.[5] In addition, we have recently shown for Fe that the metal content can be conveniently adjusted in the metallosilicate synthesis, in the range 0–11 wt%, by mixing the iron silsesquioxane and the metal-free silsesquioxane in tetrahydrofuran followed by solvent removal and calcination of the solid mixture.[7] The resulting Fe–Si–O materials showed the same good textural properties and metal dispersion as the individually calcined iron silsesquioxane. Remarkably, in this case, small iron oxide particles were the predominant iron species while mainly isolated metal species were detected previously in calcined chromium and aluminium silsesquioxanes.[5b,c] This could be related to the different propensity to hydrolysis of the M–O–Si bonds of different metallasilsesquioxanes by the water formed during calcination. The high dispersion of the metal in M–Si–O materials could therefore be associated with the low mobility of the hydrolyzed metal species, which hampers the formation of the bulk metal oxide and helps to preserve the high dispersion of the initial precursors.

Sol–gel methods can also be used to prepare mixed oxides or metal supported on silica. However, the homogeneity of the resulting multi-component materials, in terms of the distribution of various components, strongly depends on the precursors used and the preparation conditions.[8] Moreover, long gelation times are often required (*e.g.* 10 days for some silica rich gels).[9]

Bimetallic oxide catalysts are extensively used in many important industrial processes. They often perform better than their single-metal counterparts in terms of catalytic activity and/or selectivity. We report here the first application of a calcination procedure to the synthesis of a series of bimetallic Fe–Cr–Si–O materials with different Fe : Cr ratios. These were prepared by mixing a metal-free silsesquioxane, **1**, an iron silsesquioxane, **2**, and a chromium silsesquioxane, **3**.

We investigate here how the textural properties, metal speciation and dispersion of the calcined mixtures differ from the individually calcined metal silsesquioxanes. These have also been compared with a silica supported iron–chromium material prepared *via* the incipient wetness impregnation method. In order to accomplish this a set of complementary characterisation techniques including N_2 physisorption, XRD, XPS, RS, IR, HRTEM and Mössbauer spectroscopy have been used.

 DOI: 10.1039/b205051j

Experimental

Synthesis

Synthesis of silsesquioxane precursors. The incompletely condensed silsesquioxane, **1**, was prepared by the hydrolytic condensation of cyclopentyltrichlorosilane.[10] Iron and chromium silsesquioxanes, **2** and **3**, were prepared from **1** according to procedures reported earlier.[5b,7]

Synthesis of Fe–Cr–Si–O materials. Fe–Cr–Si–O materials with different Fe : Cr ratios and a total maximum metal content of 10.5 wt% were prepared by using different ratios of metal silsesquioxanes **2** and **3** (see Scheme 1). The metal-free silsesquioxane **1** was added, when necessary, in order to achieve the desired metal to silicon ratio. Hexane and toluene were used as solvents in order to dissolve the silsesquioxane precursors. Solvent removal was performed with warm solutions under a controlled vacuum and using vigorous stirring in order to ensure a good homogeneity of the resulting solid mixtures. Samples were calcined in batches of 0.5 g at 500 °C for 4 h with a flow of 20% O_2 in Ar. As reported previously for calcination of chromium and magnesium silsesquioxanes, these conditions allowed efficient carbon removal and led to materials with large surface areas.[5b,c]

A reference sample was prepared by sequential incipient wetness impregnation of a conventional mesoporous silica SG-360 Grace (surface area 513 $m^2\ g^{-1}$ and pore volume 0.95 $cm^3\ g^{-1}$). The silica was first evacuated at 200 °C for 2 h. $Fe(NO_3)_3{\cdot}9H_2O$ and CrO_3 were used as impregnation precursors. The impregnated sample was calcined under the same conditions as the silsesquioxane mixtures.

The silsesquioxane-derived samples are labeled using element symbols preceded by numbers, which indicate the approximate nominal metal contents. For example, 7/3 Fe–Cr–Si–O indicates a silica based material containing approximately 7 wt% Fe and 3 wt% Cr. The reference sample was labeled 7/3 Fe–Cr/SiO_2 (r). Fe–Si–O and Cr–Si–O indicate materials obtained from separate calcination of iron and chromium silsesquioxanes or from mixtures of these complexes with metal-free silsesquioxane. For simplicity, the silica symbol has been omitted from labels used in the figures.

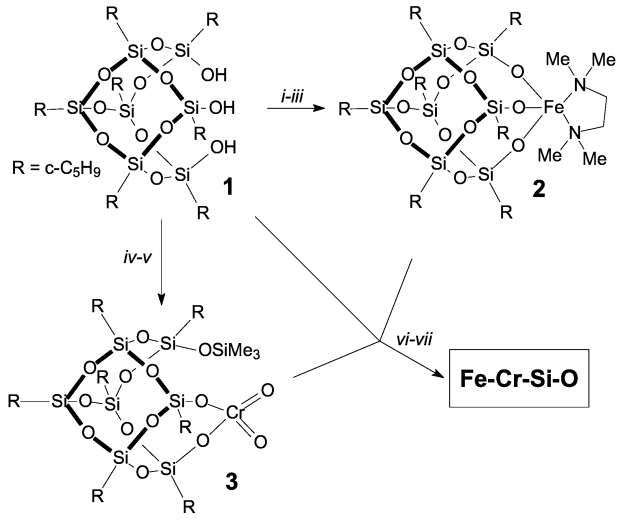

Scheme 1 A silsesquioxane route to Fe–Cr–Si–O materials with tailored metal content. *Reagents and conditions*: i: BuLi; ii: $FeCl_3$; iii: TMEDA (*N*,*N*,*N*',*N*'-tetramethylethylenediamine); iv: Me_3SiCl; v: CrO_3; vi: mixture of **1**, **2** and **3**, hexane–toluene; vii: calcination, O_2/Ar, 500 °C, 4 h.

Analysis

The carbon content of the M–Si–O materials was measured by heating the samples at 925 °C on a Perkin Elmer automated analyzer Series II CHNS/O Analyzer 2400.

Inductively coupled plasma optical emission spectrometry (ICP-OES) was used for the determination of the iron and chromium content in the Fe–Cr–Si–O materials. The measurements were taken on a SPECTRO CIROSCCD spectrometer. Before measurement the samples were dried at 110 °C for 1 h and then dissolved in an aqueous mixture of HF and HNO_3.

For nitrogen physisorption analysis, all samples were pretreated before measurement in a vacuum at 200 °C for 2 h. The measurements were performed on a Micromeritics ASAP 2000 using an equilibriation interval of 5 s and a low pressure dose of 3.00 $cm^3\ g^{-1}$ STP. Surface area, pore volume and pore size distribution of Fe–Cr–Si–O materials were calculated using the methods developed by Horvath and Kawazoe, and Dubinin and Radushkevich.[11] For the reference 7/3 Fe–Cr/SiO_2 (r) sample the BET and BJH models were used as well.[12]

X-Ray diffraction (XRD) data were collected on a Rigaku diffractometer in the range $5.0° < 2\theta < 80°$ using Cu-Kα radiation and the step scan method at 0.1 deg min^{-1} scanning speed and 5 s dwelling time.

X-Ray photoelectron spectroscopy (XPS) measurements were obtained using a VG CLAM 2 spectrometer equipped with a Mg-Kα source and a hemispherical analyzer. Measurements were carried out at 20 eV pass energy. Charging was corrected by using the Si 2p peak of SiO_2 at 103.3 eV. The samples were ground and pressed in indium foil which was placed on a stainless-steel stub. The XP spectra have been fitted using the VGS program fit routine, with a Shirley background subtraction and Gauss–Lorentz curves. The error in the binding energy was 0.2 eV. Elemental ratios were calculated from the peak areas with correction for their cross-sections.[13]

Transmission electron microscopy (TEM) was performed using a Philips CM30UT high resolution electron microscope with a field emission gun as a source of electrons operated at 300 kV. Samples were mounted on a microgrid carbon polymer supported on a copper grid by placing a few droplets of a suspension of the ground sample in ethanol or hexane on the grid followed by drying under ambient conditions.

^{57}Fe Mössbauer spectra were measured on a constant acceleration spectrometer in a triangular mode with a ^{57}Co:Rh source. Mössbauer spectra of the Fe–Cr–Si–O materials (except for 3/3 Fe–Cr–Si–O) and of the reference 7/3 Fe–Cr/SiO_2 (r) were recorded at 300, 77 and 4.2 K. The final spectra were deconvoluted using calculated Mössbauer spectra that consisted of Lorentzian-shaped lines. In the case of quadrupole doublets the linewidths and the absorption areas of the constituent lines were constrained as equal. Positional parameters were not constrained in the fitting procedure. The isomer shift values are reported relative to sodium nitroprusside, $Na_2Fe(CN)_5NO$.

Fourier transform infrared (FTIR) spectra of the Fe–Si–O samples were recorded under ambient conditions on a Nicolet Protégé 460 FTIR Spectrometer E.S.P. equipped with a MCT/A detector and a Golden Gate Single Reflection Diamond sampling unit. Automatic baseline correction of the spectra was applied.

Raman spectra were recorded on a RFS 100/S FT-Raman Bruker spectrometer. A Nd:YAG laser at 1064 nm was used as the excitation source. The measurements were made using laser powers in the range 40–180 mW. Attempts to increase the intensity of the spectra by using higher laser powers were severely limited by the intensification of the fluorescence effect. All spectra were recorded under ambient conditions by co-adding 1024 scans at a resolution of 4 cm^{-1}.

Table 1 The textural properties and composition of Fe–Cr–Si–O, Fe–Si–O, Cr–Si–O and Fe-Cr/SiO_2 (r)

Sample	Fe[a] (wt%)	Cr[a] (wt%)	Surface area[b] /m^2 g^{-1}	Pore volume[b] /ml g^{-1}	Average pore diameter[c] /Å
11% Fe–Si–O	10.6	0	623	0.22	7.0
7/3 Fe–Cr–Si–O	6.8	3	764	0.27	7.1
5/5 Fe–Cr–Si–O	5.4	4.9	569	0.20	6.7
3/6 Fe–Cr–Si–O	3.5	6.3	561	0.20	6.8
3/3 Fe–Cr–Si–O	2.9	2.6	467	0.16	6.0
10% Cr–Si–O	0	10.2	546	0.19	6.8
7/3 Fe–Cr/SiO_2 (r)[d]	6	2.8	449	0.94	80

[a]Determined by ICP-OES. [b]Estimated from the Dubinin–Radushkevich equation. [c]Estimated from the Horvath–Kawazoe equation. [d]For this sample, the surface area was estimated from the BET equation and pore volume and average pore diameter from the BJH equation.

Results and discussion

The nominal and actual metal bulk content of the Fe–Cr–Si–O materials and of the 7/3 Fe–Cr/SiO_2 (r) reference sample are shown in Table 1. The actual metal contents were analysed by ICP-OES and deviate slightly from the expected values. Unless otherwise notified, all metal loadings mentioned in the paper are referred to the nominal values. The average carbon content of the Fe–Cr–Si–O materials determined by elemental analysis was about 0.1 wt%.

The textural properties of the Fe–Cr–Si–O materials and of the reference sample were determined by N_2 physisorption. All of the Fe–Cr–Si–O samples yielded type Ib isotherms characteristic of microporous materials. The reference sample showed a type IV isotherm associated with a small increase in the adsorption amount at low p/p_0. This indicates a mesoporous material also containing a small amount of micropores. The assignment of the materials' isotherms was made according to the extended IUPAC classification.[14]

Typical values for surface area, pore volume and average pore diameter for Fe–Cr–Si–O, Fe–Si–O, Cr–Si–O samples and the reference are presented in Table 1. These results indicate that the calcination of the metal silsesquioxane mixtures produced microporous materials with large surface areas of about 450–750 m^2 g^{-1}, rather large pore volumes of about 0.16–0.27 ml g^{-1} and a narrow pore size distribution with an average pore size diameter around of 6–7 Å. These results are comparable with those observed for individually calcined metal silsesquioxanes.[5b,7] The reference sample showed a surface area of 449 m^2 g^{-1}, a very large pore volume of 0.94 ml g^{-1} and an average pore diameter around of 80 Å. These values correspond closely to those observed for the non-impregnated silica support. This is to be expected since the morphology of the supported samples is dictated to a large extent by the supports used.

The metal dispersion in Fe–Cr–Si–O materials and in the reference 7/3 Fe-Cr/SiO_2 (r) was estimated from XPS data. The surface Fe : Si, Cr : Si and Fe : Cr atomic ratios obtained by XPS analysis are presented in Table 2. The surface Fe : Si ratios are similar to the bulk ratios for all Fe–Cr–Si–O samples indicating a high dispersion of iron in these materials. The surface Fe : Si ratio of the reference sample is half of the bulk ratio. This means that in the reference sample the iron might be present in the form of large particles of probably iron oxide.

Table 2 Surface (XPS) and bulk (ICP) atomic ratios for Fe–Cr–Si–O and Fe–Cr/SiO_2 (r)

	Fe : Si		Cr : Si		Fe : Cr	
Sample	Surface	Bulk	Surface	Bulk	Surface	Bulk
7/3 Fe–Cr–Si–O	0.075	0.086	0.068	0.041	1.102	2.11
5/5 Fe–Cr–Si–O	0.069	0.070	0.095	0.068	0.728	1.02
3/6 Fe–Cr–Si–O	0.048	0.045	0.130	0.087	0.371	0.51
3/3 Fe–Cr–Si–O	0.043	0.034	0.062	0.033	0.685	1.03
7/3 Fe–Cr/SiO_2 (r)	0.038	0.075	0.053	0.037	0.726	1.99

The surface Cr : Si ratios of both the Fe–Cr–Si–O and the reference samples indicate a less uniform distribution of the chromium. The surface Cr : Si ratio is higher than the bulk ratio indicating that the chromium resides preferentially on the silica surface than in the bulk. Consequently, the surface Fe : Cr ratios are lower than the expected bulk values for all the samples with a markedly decreased value for the reference sample, 0.726 instead of 1.99. Comparison between the 7/3 Fe–Cr–Si–O sample and the reference indicates a better metal dispersion for the silesquioxane-derived sample. It also suggests that the iron and chromium species are much better interdispersed in the Fe–Cr–Si–O samples than in the reference.

Raman spectroscopy can provide useful information about the metal oxide speciation in oxide materials. Raman spectra of Fe–Cr–Si–O materials with various metal loadings, measured under ambient conditions, are presented in Fig. 1. For comparison, Raman spectra of 5% Fe–Si–O, 10% Cr–Si–O and of silica obtained by calcination of metal-free silsesquioxane **1** are shown as well. The silica possesses weak Raman bands at ~487, ~600, ~802 and 993 cm^{-1}. The 993 cm^{-1} band is associated with the Si–OH stretching mode of the surface hydroxys. The broad bands at 600 and 487 cm^{-1} are attributed to vibration modes of tri- and tetracyclosiloxane rings produced *via* the condensation of surface hydroxys.[15] The band at ~802 cm^{-1} has been assigned to the symmetrical Si–O–Si stretching mode.[16] The 5% Fe–Si–O sample does not show any Raman bands characteristic of iron oxide. However, we have recently shown that such a sample does contain very small and highly dispersed γ-Fe_2O_3 (maghemite) particles.[7] This is explained by the fact that the Raman bands of maghemite are not well defined and their resolution seems to depend on the degree of crystallinity of the material. The Cr–Si–O sample shows two rather well-defined bands at 980

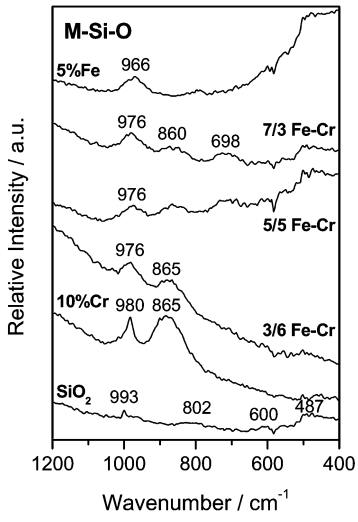

Fig. 1 Raman spectra of the Fe–Cr–Si–O, Fe–Si–O and Cr–Si–O materials.

and 865 cm^{-1} assigned to dehydrated and hydrated monochromate species, respectively.[17] The Fe–Cr–Si–O samples show also the hydrated monochromate band, which becomes less defined as the chromium content decreases. The band at 980 cm^{-1} is broadened and slightly shifted to 976 cm^{-1} and it could be due to both the dehydrated monochromate species and the silica. However, accurate determination of the position of these bands is hindered by the low intensity of the spectra and the fluorescence arising from the background of the samples. For the same reasons, the presence of other chromium oxide species such as dichromates, trichromates or Cr_2O_3 cannot be ruled out.

Remarkably, a new band is observed at $\sim$698 cm^{-1} for the 7/3 and 5/5 Fe–Cr–Si–O samples. The intensity of this band is higher for the former sample that has the highest content of iron. This band is not present in the Raman spectra of Fe–Si–O and Cr–Si–O materials, suggesting that it might be attributed to an iron–chromium mixed oxide phase. Note that a band appearing in the 650–700 cm^{-1} range was reported in the literature for spinel type iron–chromium mixed oxides.[18] The 698 cm^{-1} band is not observed in the Raman spectrum of the 3/6 Fe–Cr–Si–O sample. A possible explanation for the absence of this band is proposed in the Mössbauer analysis section.

Raman spectra of the reference 7/3 Fe-Cr/SiO_2 (r) sample and of the silica used for the impregnation, measured under ambient conditions, are shown in Fig. 2. The silica possesses Raman bands at $\sim$487, $\sim$600, $\sim$804 and 966 cm^{-1}, which have been assigned already. The bimetallic reference sample shows the dehydrated and hydrated monochromate bands at 980 and 872 cm^{-1}, respectively. In addition, three narrow bands are observed at 409, 292 and 224 cm^{-1}, which are assigned in accord with previous reports to a α-Fe_2O_3 (hematite) phase.[19] Note that in contrast to maghemite the Raman spectrum of hematite is characterized by sharp and intense bands, which makes this phase easier to detect. Moreover, no band is observed in the $\sim$650–700 cm^{-1} range where bimetallic mixed oxide phases have been reported.[18]

The XPS and Raman spectra suggest that in the Fe–Cr–Si–O materials the metal oxide species are highly interdispersed and can come into close contact with each other during the calcination procedure thus favoring the formation of the bimetallic mixed oxide phase. The absence of such a phase in the reference sample might be attributed to a poor interdispersion of the chromium and iron oxide species.

Additional information about chromium speciation was obtained from IR spectroscopy. The IR spectra of 3/6, 5/5 and 7/3 Fe–Cr–Si–O, 7/3 Fe-Cr/SiO_2 (r) and of silica prepared by calcination of metal-free silsesquioxane **1**, were measured under ambient conditions and are shown in Fig. 3. Pure silica exhibits the symmetrical Si–O–Si stretching vibration at $\sim$803 cm^{-1}, along with a band at $\sim$968 cm^{-1} due to the symmetric stretch of Si–OH groups.[20] The $\sim$968 cm^{-1} band has a shoulder at about $\sim$910 cm^{-1} for all the chromium containing samples. This shoulder is not observed in the IR spectra of silica or the Fe–Si–O sample (this spectrum is not shown for the sake of brevity). Comparison with literature data suggests that dichromates are also present on the surface of the iron–chromium containing samples as these species alone absorb in the 900–950 cm^{-1} range.[21]

The chemical state of iron in the Fe–Cr–Si–O materials and in the reference sample was also investigated by means of Mössbauer spectroscopy. Mössbauer spectra were recorded at 300 K, 77 K and 4.2 K. For the sake of brevity only the spectra recorded at 4.2 K are shown in Fig. 4. The parameters of all Mössbauer measurements are included in Table 3. The Mössbauer spectra recorded at 300 K and 77 K of the Fe–Cr–Si–O materials all show a quadrupole doublet with

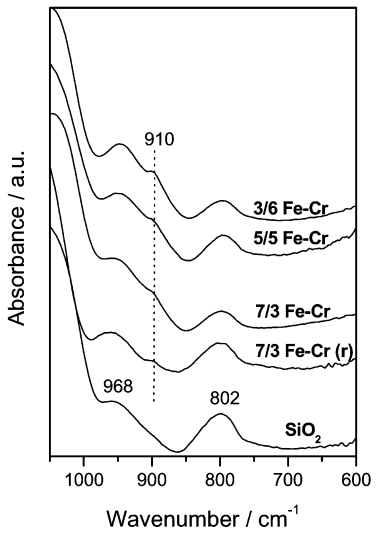

Fig. 3 Infrared spectra of the Fe–Cr–Si–O materials and the Fe–Cr/SiO_2 (r) reference sample.

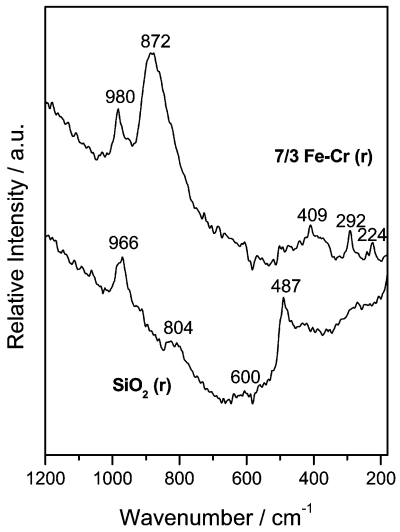

Fig. 2 Raman spectra of the Fe–Cr/SiO_2 (r) reference sample and of silica.

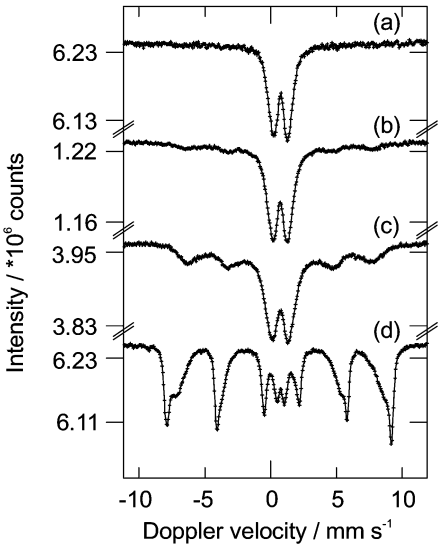

Fig. 4 ^{57}Fe Mössbauer spectra recorded at 4.2 K for (a) 3/6 Fe–Cr–Si–O, (b) 5/5 Fe–Cr–Si–O, (c) 7/3 Fe–Cr–Si–O and (d) 7/3 Fe–Cr/SiO_2 (r).

Table 3 Mössbauer parameters of the Fe–Cr–Si–O materials and the 7/3 Fe–Cr/SiO_2 (r) reference

Material	Temperature/K	Isomer shift/mm s^{-1}	Quadrupole splitting/mm s^{-1}	Hyperfine field/T	Spectral contribution (%)
3/6 Fe–Cr–Si–O	300	0.62	1.12		100
	77	0.73	1.12		100
	4.2	0.73	1.15		100
5/5 Fe–Cr–Si–O	300	0.61	1.10		100
	77	0.72	1.12		100
	4.2	0.73	1.19		24
		0.71	0.00	43.0	76
7/3 Fe–Cr–Si–O	300	0.60	1.09		100
	77	0.71	1.15		100
	4.2	0.71	1.31		48
		0.72	0.02	43.4	52
7/3 Fe–Cr/SiO_2 (r)	300	0.60	0.70		78
		0.63	0.10	48.7	22
	77	0.73	0.72		64
		0.74	0.10	52.3	36
	4.2	0.77	0.61		15
		0.75	0.11	53.1	28
		0.74	0.03	48.0	57

spectral parameters that indicate a high-spin Fe^{3+} state. At 4.2 K, however, differences appear in the spectra. Whereas the 3/6 Fe–Cr–Si–O sample (Fig. 4a) shows only a quadrupole doublet, the 5/5 and 7/3 Fe–Cr–Si–O materials (Fig. 4b and c) reveal both a quadrupole doublet and a magnetic component, which is composed of six lines. The Mössbauer spectra recorded for the reference material, 7/3-Fe-Cr/SiO_2 (r), (Fig. 4 d) present a different view. Most significantly, the spectrum of this material, which was recorded at 300 K, shows a quadrupole doublet with spectral parameters that differ strongly from the parameters determined for the doublets found in the 300 K spectra of the Fe–Cr–Si–O materials. In addition to the quadrupole doublet, a sextuplet with well-defined lines is observed. This magnetic component, which grows in intensity at lower temperatures, has spectral parameters that strongly indicate the presence of large α-Fe_2O_3 particles. Moreover, a second magnetic component with less well-defined lines is observed at 4.2 K. This component with an average hyperfine field of *ca.* 48 T most likely belongs to small iron oxide particles, which vary in size from 2 to 4 nm and have more amorphous character than the aforementioned α-Fe_2O_3 particles.

These measurements clearly indicate that different iron-containing phases are formed, depending on the method of preparation. Whereas the method of impregnation of mesoporous silica leads to a rather inhomogeneous mixture of different iron oxide clusters, the method based on silsesquioxane precursors leads to a more homogeneous phase. This phase is most likely a solid solution of α-Fe_2O_3 and Cr_2O_3 oxides. It is known that the crystal structures of these phases are the same and that they can mix easily.[22] Such a mixed oxide is more likely to be formed than a spinel phase, since the latter would require Fe^{2+} ions, which have not been observed in the Mössbauer spectra. Note also that besides monochromate species very small clusters of Cr_2O_3 were detected by Raman spectroscopy in the calcined chromium silsesquioxane **3**.[5b] The formation of a mixed oxide is indicated by the presence of a magnetic component in the Mössbauer spectra of 5/5 Fe–Cr–Si–O and 7/3 Fe–Cr–Si–O materials that were measured at 4.2 K (Fig. 4b and c). This magnetic component has a hyperfine field close to 43 T, which is too small for an iron oxide phase. It is known that an increasing amount of Cr_2O_3 in a α-Fe_2O_3 phase leads to a reduction in the observed hyperfine field.[23] Because TEM indicates that there is no difference in the sizes of the metal oxide particles observed for the different Fe–Cr–Si–O materials, we attribute the differences in intensity of the magnetic component observed in the 4.2 K Mössbauer spectra to variations in the Fe : Cr ratio in these oxides. This could also explain the disappearance of the 698 cm^{-1} Raman band from the spectra of 3/6 Fe–Cr–Si–O sample.

Electron microscopy is a widely used technique that can provide information about the dispersion and size of metal oxide particles on a support surface. Examination of the Fe–Cr–Si–O materials and of the 7/3 Fe-Cr/SiO_2 (r) reference with high resolution TEM yielded images that confirm the presence of metal oxide particles on the silica surface. The Fe–Cr–Si–O samples showed very small and well dispersed metal oxide particles of about 2–4 nm size as exemplified in Fig. 5a for 7/3 Fe–Cr–Si–O. In contrast, large and non-uniformly dispersed crystalline particles of about 10–30 nm can be observed on the reference sample, as shown in Fig. 5b. No lattice fringes could be observed for the metal oxide particles present on the 7/3 Fe–Cr–Si–O sample suggesting that they have an amorphous character. According to the Raman and Mössbauer spectra these small particles should consist of a bimetallic mixed oxide phase. The presence of particles on the 3/6 Fe–Cr–Si–O sample (not shown here for the sake of brevity) and the absence of a magnetic sextuplet in the 4.2 K Mössbauer spectrum of this sample indicate that the particles consist in this case of a non-magnetic metallic oxide phase. This phase is probably also a bimetallic mixed oxide since no particles were observed by TEM on the surface of a 10% Cr–Si–O material and a 3% Fe–Si–O material did show a magnetic sextuplet in the 4.2 K Mössbauer spectrum.[7]

The large crystalline particles present on the surface of the reference sample allowed us to measure the lattice fringe spacings and the values obtained (d = 1.59, 2.68, 3.70 Å) indicate a good fit with the α-Fe_2O_3 (hematite) phase (d = 1.59, 2.69, 3.68 Å, JCPDS file No. 86-0550). This finding is in

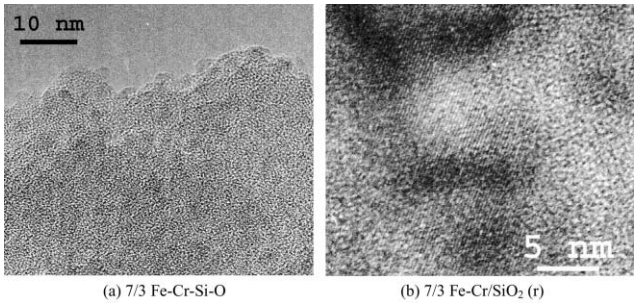

Fig. 5 TEM micrographs of (a) 7/3 Fe–Cr–Si–O and (b) 7/3 Fe–Cr/SiO_2 (r).

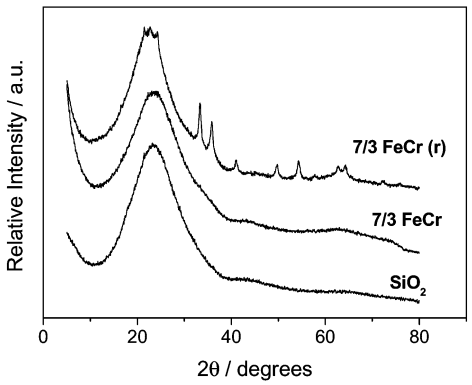

Fig. 6 XRD patterns of 7/3 Fe–Cr/SiO_2 (r), 7/3 Fe–Cr–Si–O and silica.

agreement with Raman and Mössbauer spectra of the reference sample.

As expected, these large hematite particles were also visible in the XRD pattern of the reference sample, as shown in Fig. 6. In this case, sharp peaks are observed at 33.27, 35.83, 40.96, 49.73, 54.28, 62.61 and 64.31° 2θ angles, which are typical for hematite. The average diameter of these particles estimated from line broadening analysis is 21 nm, which is in the size range observed with TEM. The XRD patterns of 7/3 Fe–Cr–Si–O and of silsesquioxane derived silica, shown also in Fig. 6 for comparison, show only a broad band at around 20–30° 2θ angle, which is usually assigned to amorphous silica.[24] This is to be expected for the 7/3 Fe–Cr–Si–O sample since the bimetallic mixed oxide particles observed with TEM seem to be amorphous.

The TEM and XRD results are in good agreement with Raman and Mössbauer spectra. Together, they indicate the formation of bimetallic mixed oxide particles in silsesquioxane-derived Fe–Cr–Si–O materials and the formation of separate iron oxide particles and chromate species in the impregnated Fe-Cr/SiO_2 (r) reference sample.

These results suggest that metallasilsesquioxane mixtures may be used as versatile precursors for the preparation of silica-based catalysts containing very small and well dispersed particles of mixed metal oxides. Moreover, the solubility of these metallasilsesquioxane precursors in organic solvents and the ability to fine tune the resulting material composition make this novel preparation method suitable to automatization and a combinatorial approach.

Conclusions

Microporous amorphous bimetallic Fe–Cr–Si–O materials with different metal ratios were prepared by calcination of silsesquioxane mixtures of **1**, **2**, and **3**. The variation of the textural properties, metal dispersion and speciation with metal content were investigated by various complementary techniques.

Fe–Cr–Si–O materials possess high surface areas and uniformly controlled micropores with an average pore size diameter of around 6–7 Å. Metal oxide speciation appears to be significantly different from the one observed for these metals in the individually calcined metal silsesquioxanes. Iron oxide and monochromates, respectively, are the predominant species in the calcined **2** and **3** precursors while very small particles (2–4 nm) of bimetallic mixed oxides are the major species in Fe–Cr–Si–O materials. This suggests that the metal oxide species are highly interdispersed and can come into close contact with each other during the calcination procedure thus favoring the formation of the bimetallic mixed oxide phase. In contrast, a silica reference material containing 7% Fe and 3% Cr prepared *via* impregnation showed only chromate species and large particles (10–30 nm) of iron oxide.

These results indicate that metallasilsesquioxane mixtures may be used as versatile precursors for the preparation of silica-based catalysts containing very small and well dispersed particles of mixed metal oxides. Moreover, this method seems to be suitable to automatization and a combinatorial approach.

Acknowledgements

This work was supported in part (NM, HCLA, PJK) by the Council for Chemical Sciences of the Netherlands Organization for Scientific Research (NWO-CW) and by Avantium Technologies company (NM, HCLA). Ing. M. W. G. M. Verhoeven is gratefully acknowledged for his support with the XPS and Ms A. M. Elemans-Mehring for OES-ICP measurements.

References

1 (*a*) R. H. Baney, M. Itoh, A. Sakakibara and T. Suzuki, *Chem. Rev.*, 1995, **95**, 1409; (*b*) P. A. Agaskar, *Chem. Commun.*, 1992, 1024; (*c*) R. A. Mantz, P. F. Jones, K. P. Chaffee, J. D. Lichtenhan and J. W. Gilman, *Chem. Mater.*, 1996, **8**, 1250.
2 F. J. Feher and T. A. Budzichowski, *Polyhedron*, 1995, **14**, 3239.
3 (*a*) T. Maschmeyer, M. C. Klunduk, C. M. Martin, D. S. Shephard, J. M. Thomas and B. F. G. Johnson, *Chem. Commun.*, 1997, 1847; (*b*) M. Crocker, R. H. M. Herold and A. G. Orpen, *Chem. Commun.*, 1997, 2411.
4 (*a*) R. Duchateau, H. C. L. Abbenhuis, R. A. van Santen, A. Meetsma, S. K. H. Thiele and M. F. H. van Tol, *Organometallics*, 1998, **17**, 5663; (*b*) R. Duchateau, U. Cremer, R. J. Harmsen, S. I. Mohamud, H. C. L. Abbenhuis, R. A. van Santen, A. Meetsma, S. K. H. Thiele, M. F. H. van Tol and M. Kranenburg, *Organometallics*, 1999, **18**, 5447.
5 (*a*) K. Wada, M. Nakashita, M. Bundo, K. Ito, T. Kondo and T. Mitsudo, *Chem. Lett.*, 1998, 659; (*b*) N. Maxim, H. C. L. Abbenhuis, P. J. Stobbelaar, B. L. Mojet and R. A. van Santen, *Phys. Chem. Chem. Phys.*, 1999, **1**, 4473; (*c*) N. Maxim, P. C. M. M. Magusin, P. J. Kooyman, J. H. M. C. van Wolput, R. A. van Santen and H. C. L. Abbenhuis, *Chem. Mater.*, 2001, **13**, 2958; (*d*) K. Wada, K. Yamada, T. Kondo and T. Mitsudo, *Chem. Lett.*, **2001**, 12.
6 (*a*) M. G. Voronkov and V. I. Lavrent'yev, *Top. Curr. Chem.*, 1982, **102**, 199; (*b*) V. Lorenz, A. Fischer, S. Giebmann, J. W. Gilje, Y. Gun'ko, K. Jacob and F. T. Edelmann, *Coord. Chem. Rev.*, 2000, **206-207**, 321; (*c*) H. C. L. Abbenhuis, *Chem. Eur. J.*, 2000, **6**, 25.
7 N. Maxim, A. Overweg, P. J. Kooyman, J. H. M. C. van Wolput, R. W. J. M. Hanssen, R. A. van Santen and H. C. L. Abbenhuis, *J. Phys. Chem. B*, 2002, **106**, 2203.
8 (*a*) H. H. Kung and E. I. Ko, *Chem. Eng. J.*, 1996, **64**, 203; (*b*) H. Hutter, T. Mallat and A. Baiker, *J. Catal.*, 1995, **153**, 177.
9 (*a*) J. Klein, C. Lettmann and W. F. Maier, *J. Non-Cryst. Solids*, 2001, **282**, 203; (*b*) J. D. Mackenzie, in *Sol-Gel Science and Technology*, American Chemical Society, Ohio, 1997.
10 F. J. Feher, T. A. Budzichowski, R. L. Blanski, K. J. Weller and J. W. Ziller, *Organometallics*, 1991, **10**, 2526.
11 (*a*) M. M. Dubinin and L. V. Radushkevich, *Proc. Acad. Sci. USSR*, 1947, **55**, 331; (*b*) G. Horvath and K. Kawazoe, *J. Chem. Eng. Jpn.*, 1983, **16**, 470.
12 (*a*) S. Brunauer, P. H. Emmett and E. Teller, *J. Am. Chem. Soc.*, 1938, **60**, 309; (*b*) E. P. Barrett, L. G. Joyner and P. P. Halenda, *J. Am. Chem. Soc.*, 1951, **73**, 373.
13 J. H. Scofield, *J. Electron Spectrosc. Relat. Phenom.*, 1976, **8**, 129.
14 F. Rouquerol, J. Rouquerol and K. Sing, in *Adsorption by Powders & Porous Solids – Principles, Methodology and Applications*, Academic Press, London, 1999.
15 (*a*) B. A. Morrow and A. J. Mcfarlan, *J. Non-Cryst. Solids*, 1990, **120**, 61; (*b*) C. J. Brinker, R. J. Kirkpatrick, D. R. Tallant, B. C. Bunker and B. Montez, *J. Non-Cryst. Solids*, 1988, **99**, 418.
16 P. MacMillan, *Am. Mineral.*, 1986, **69**, 622.
17 (*a*) B. M. Weckhuysen, I. E. Wachs and R. A. Schoonheydt, *Chem. Rev.*, 1996, **96**, 3327; (*b*) F. D. Hardcastle and I. E. Wachs, *J. Mol. Catal.*, 1988, **46**, 173; (*c*) D. S. Kim, J. M. Tatibouet and I. E. Wachs, *J. Catal.*, 1992, **136**, 209.
18 (*a*) S. C. Tjong, *Mater. Characteriz.*, 1991, **26**, 29; (*b*) P. Fabis, R. Heiderbach, C. Brown and T. Rockett, *Corrosion*, 1981, **37**, 700.

19 (*a*) D. L. A. de Faria, S. V. Silva and M. T. de Oliveira, *J. Raman Spectrosc.*, 1997, **28**, 873; (*b*) F. Perez-Robles, F. J. Garcia-Rodriguez, S. Jimenez-Sandoval and J. Gonzales-Hernandez, *J. Raman Spectrosc.*, 1999, **30**, 1099.
20 (*a*) M. R. Boccuti, K. M. Rao, A. Zecchina, G. Leofanti and G. Petrini, *Stud. Surf. Sci. Catal.*, 1989, **48**, 133; (*b*) A. Zecchina, S. Bordiga, S. Spoto, L. Marchese, G. Petrini, G. Leofanti and M. Padovan, *J. Phys. Chem.*, 1992, **96**, 4985.
21 (*a*) A. Zecchina, E. Garrone, G. Ghiotti, C. Morterra and E. Borello, *J. Phys. Chem.*, 1975, **79**, 966; (*b*) H. Stammreich, D. Sala and K. Kawai, *Spectrochim. Acta*, 1961, **17**, 226.
22 T. C. Gibb and N. N. Greenwood, in *Mössbauer Spectroscopy*, Chapman and Hall Ltd., London, 1971.
23 G. Shirane, D. E. Cox and S. L. Ruby, *Phys. Rev.*, 1962, **125**, 1158.
24 C. Real, M. D. Alcala and J. M. Criado, *J. Am. Ceram. Soc.*, 1996, **79**, 2012.